On the possibility to count fast neutrons with high spatial and timing resolution

A.S. Tremsin

University of California at Berkeley, Berkeley, CA 94720, USA

in collaboration with

Nova Scientific
(thermal and epithermal neutron detection)
10 Picker Rd., Sturbridge, MA 01566, USA

Arradiance (fast neutron detection)
142 North Road, Suite F-150, Sudbury, MA 01776, USA

Many beamline scientists at neutron facilities and
Medipix collaboration

The work done in collaboration

CERN Medipix team
Advacam
NIKHEF, Amsterdam
IEAP, Prague
University of California at Berkeley, CA, USA
A.S. Tremsin, J. B. McPhate, J. V. Vallerga, O. H. W. Siegmund
Nova Scientific, Inc, Sturbridge, USA (manufacturer of neutron sensitive MCPs)
W. B. Feller, P. White, B. White
Rutherford Appleton Laboratory, ISIS Facility, UK
W. Kockelmann, J. Kelleher, S. Kabra, D.E. Pooley, G. Burca, T. Minniti, E. Schooneveld, N. Rhodes
J-PARC Center, JAEA, Nagoya University, Japan
Y. Kiyanagi, T. Shinohara. T. Kai, K. Oikawa
LANSCE, Los Alamos National Laboratory
S. Vogel, A. Losko, M. Mocko, M.A.M. Bourke, R. Nelson
Paul Scherrer Institute, Switzerland
E. Lehmann, A. Kaestner, T. Panzner, P. Trtik, M. Mangano
Istituto dei Sistemi Complessi, Sesto Fiorentino (FI), Italy
F. Grazzi
ANSTO
A. Sokolova, A. Paradowska, V. Luzin, F. Salvemini
CONICET and Instituto Balseiro, Centro Atomico Bariloche, Argentina
J. Santisteban
Spallation Neutron Source, Oak Ridge National Laboratory, USA
H. Z. Bilheux, L.J. Santodonato
Technische Universität München, Forschungs-Neutronenquelle FRM-II, Germany
B. Schillinger, M. Lerche
Department of Geology and Environmental Earth Science, Miami University
John Rakovan
Welding Science, Cranfield University
Supriyo Ganguly
University of Newcastle, Latrobe University, Australia
C. Wensrich, E. Kisi. H. Kirkwood

Lawrence Berkeley Laboratory
D. Perrodin, G.A. Bizarri, E.D. Bourret
European Spallation Source Scandinavia
M. Strobl, R. Woracek
Technical University of Denmark
S. Schmidt
Open University, Coventry University, UK
M. Fitzpatrick, R. Ramadhan
General Electric Global Research
Yan Gao

…and many others!
apologies for missed names

MCP electron amplifier for UV/neutron detection

Circular pores ~8 μm ∅

Walls between pores ~2 μm

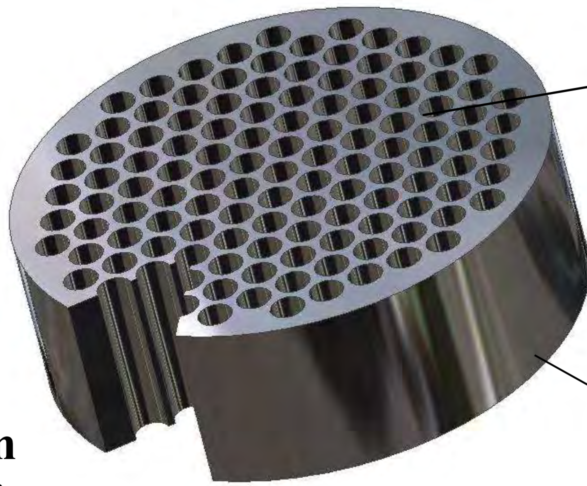

~1 mm absorption length

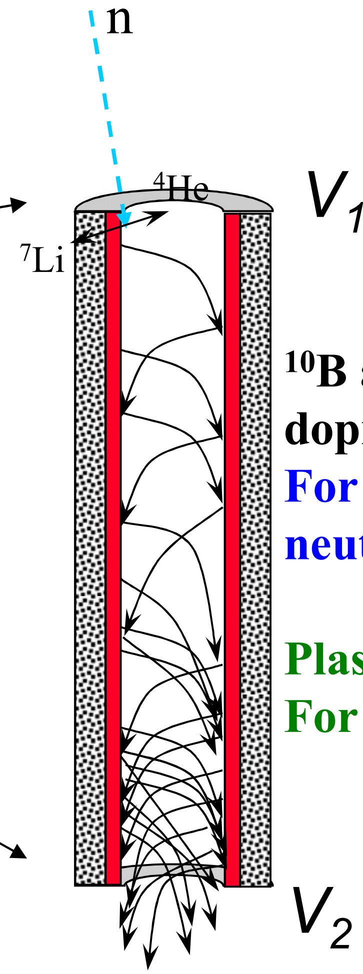

^{10}B and Gd doping in glass

For thermal neutron detection;

Plastic MCP For fast neutrons

1 mm absorption length

~2 μm escape range

High detection efficiency!!

Single pore

MCP/Timepix detector for neutron imaging: principle of operation

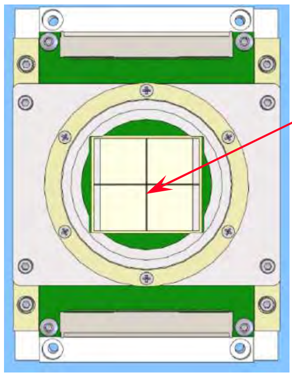

- Active area with 2x2 Timepix chips (28x28 mm^2)
- Fast parallel readout (x32) allowing ~1200 frames per second and ~300 μs dead time
- Wide transmission spectrum measured at the same time.

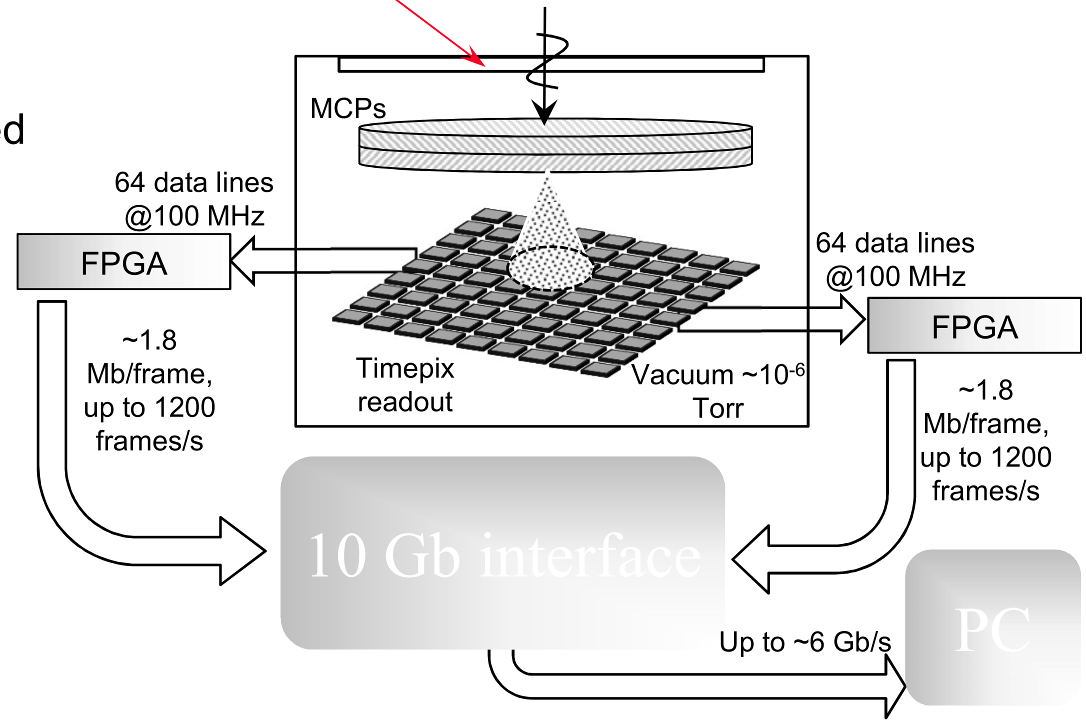

A.S. Tremsin, et al., NIM A **787** (2015) 20–25.

Time resolved imaging and imaging of cyclic dynamic processes

Quantification of water dynamics

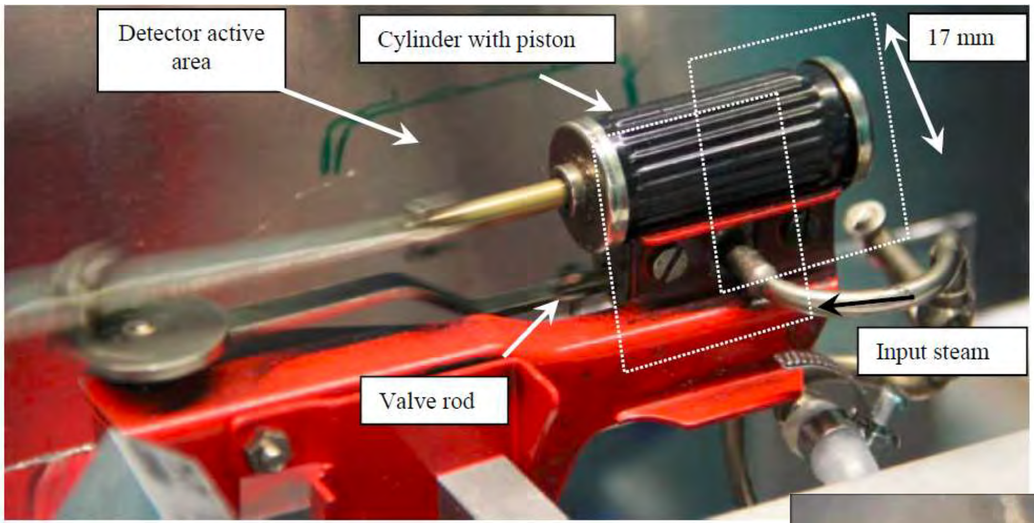

Toy steam engine cylinder @ 10 Hz

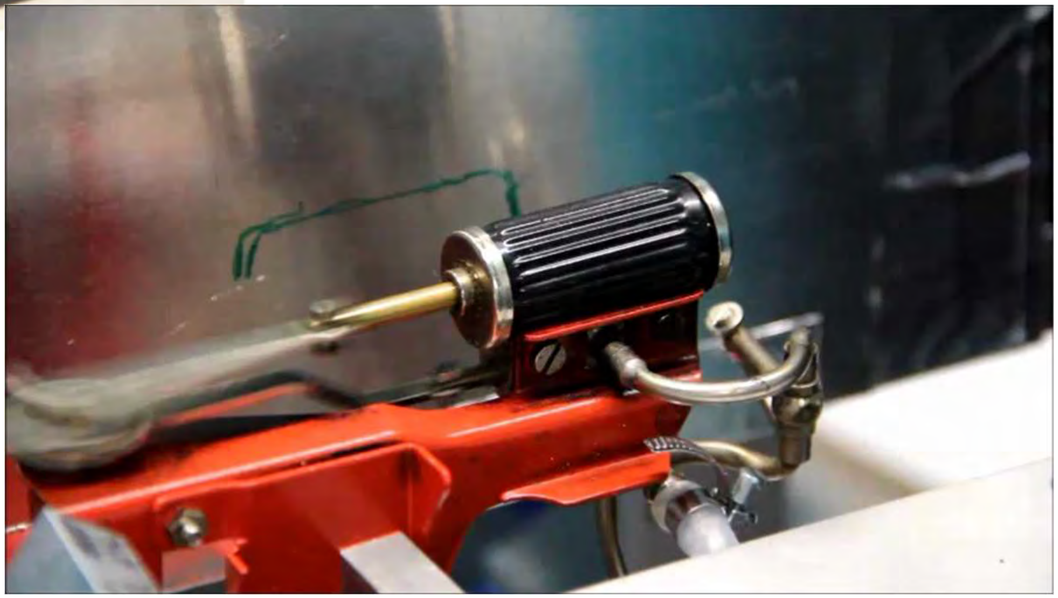

Quantification of water dynamics

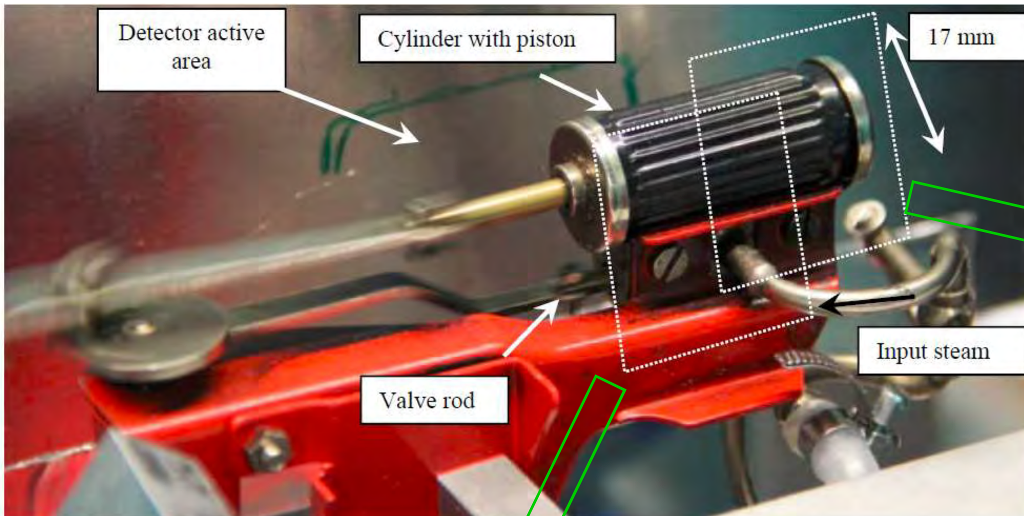

Dry cylinder operation
(1 ms time slice)

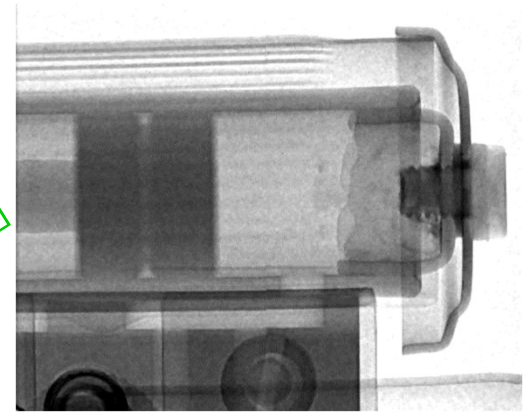

Operation with steam
(1 ms time slice)

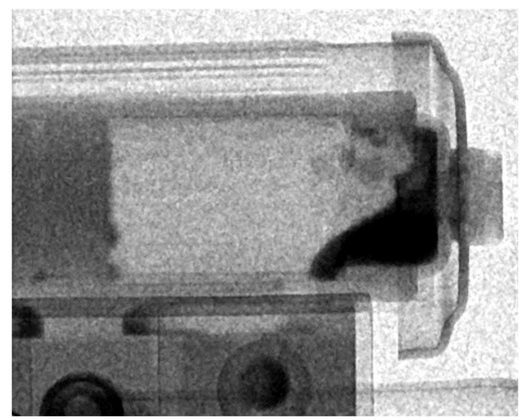

Dry cylinder operation
(1 ms time slice)

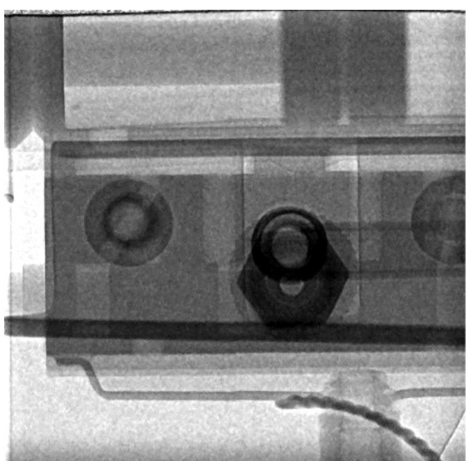

Operation with steam
(1 ms time slice)

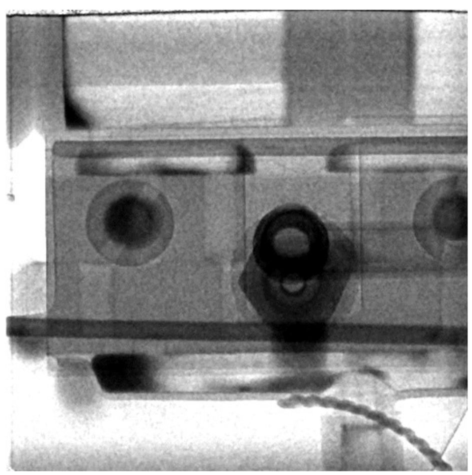

Quantification of water dynamics

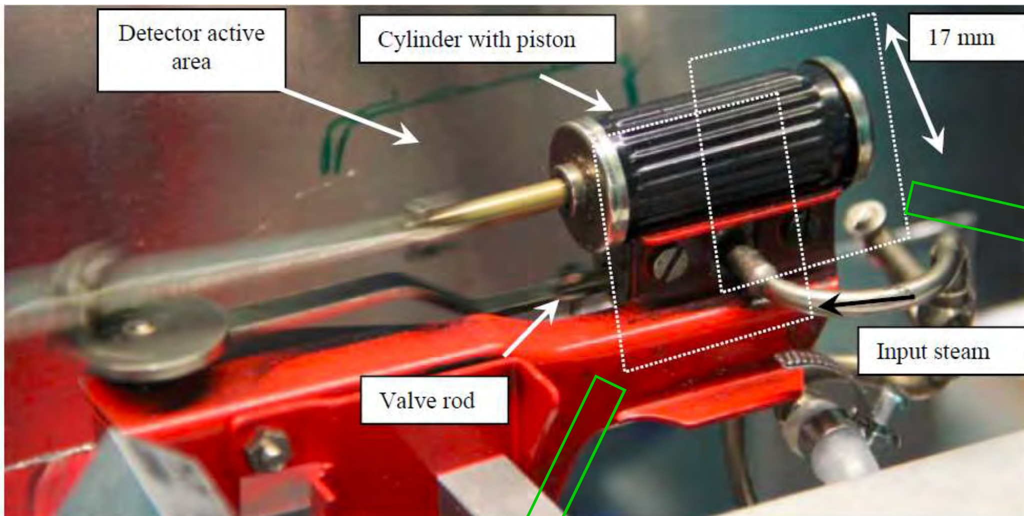

Images of water only
1 ms slices

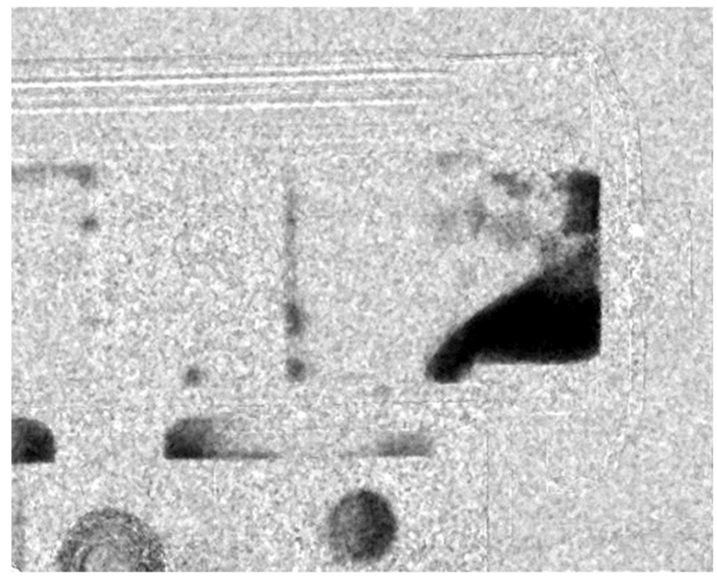

Leaking valve: a droplet is formed in each cycle

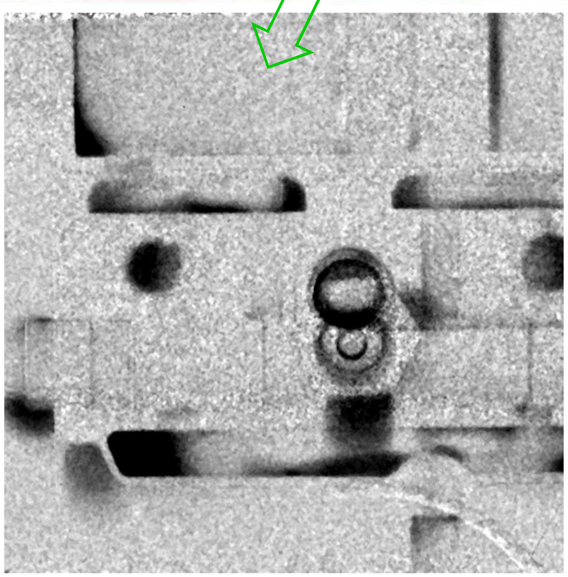

JINST 10 (2015) P07008

Quantification of water in cylinder

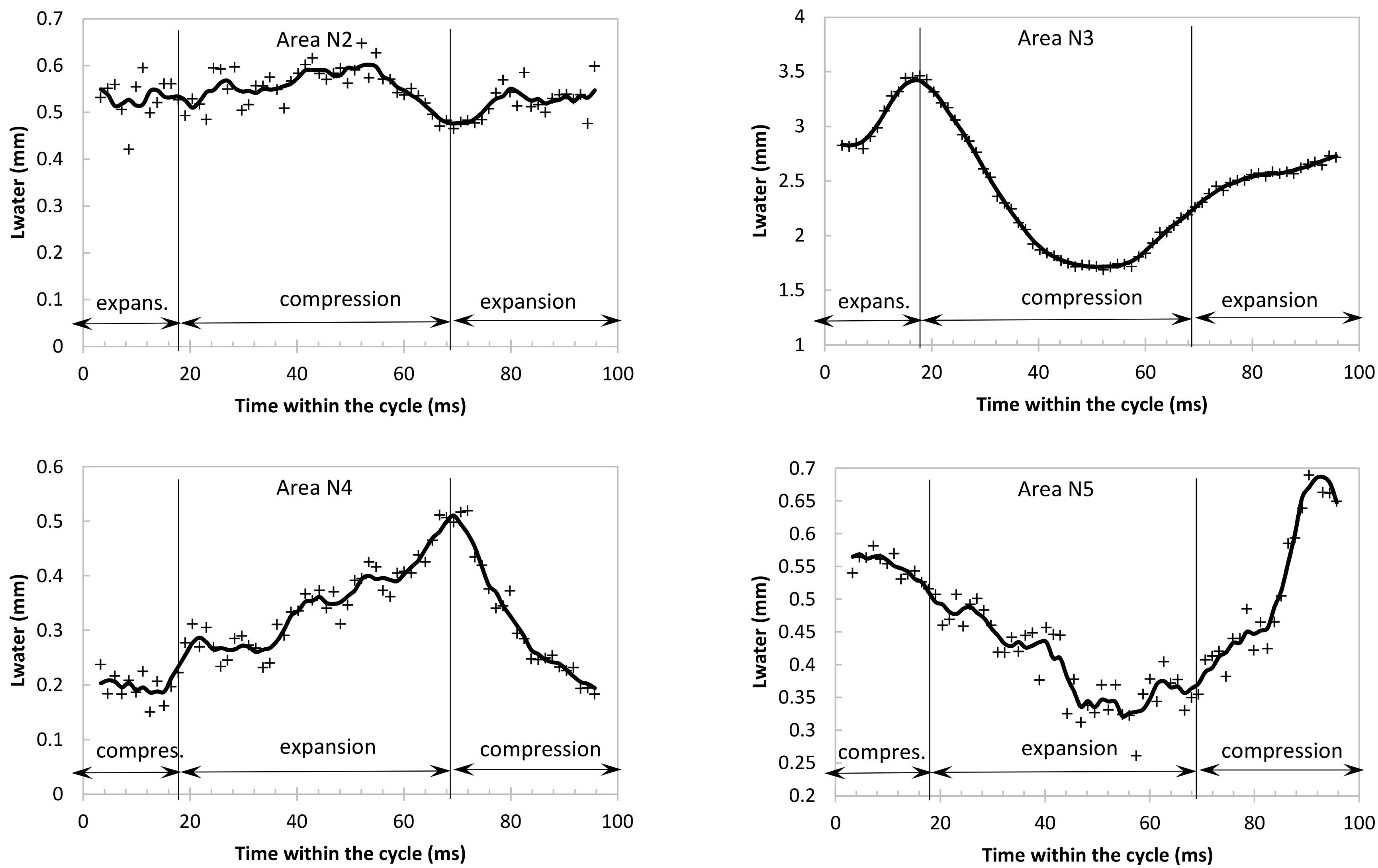

Fast neutron imaging workshop, Garching, Oct. 2019

Water quantification as a function of time within the cycle

Water thickness averaged
over all phases

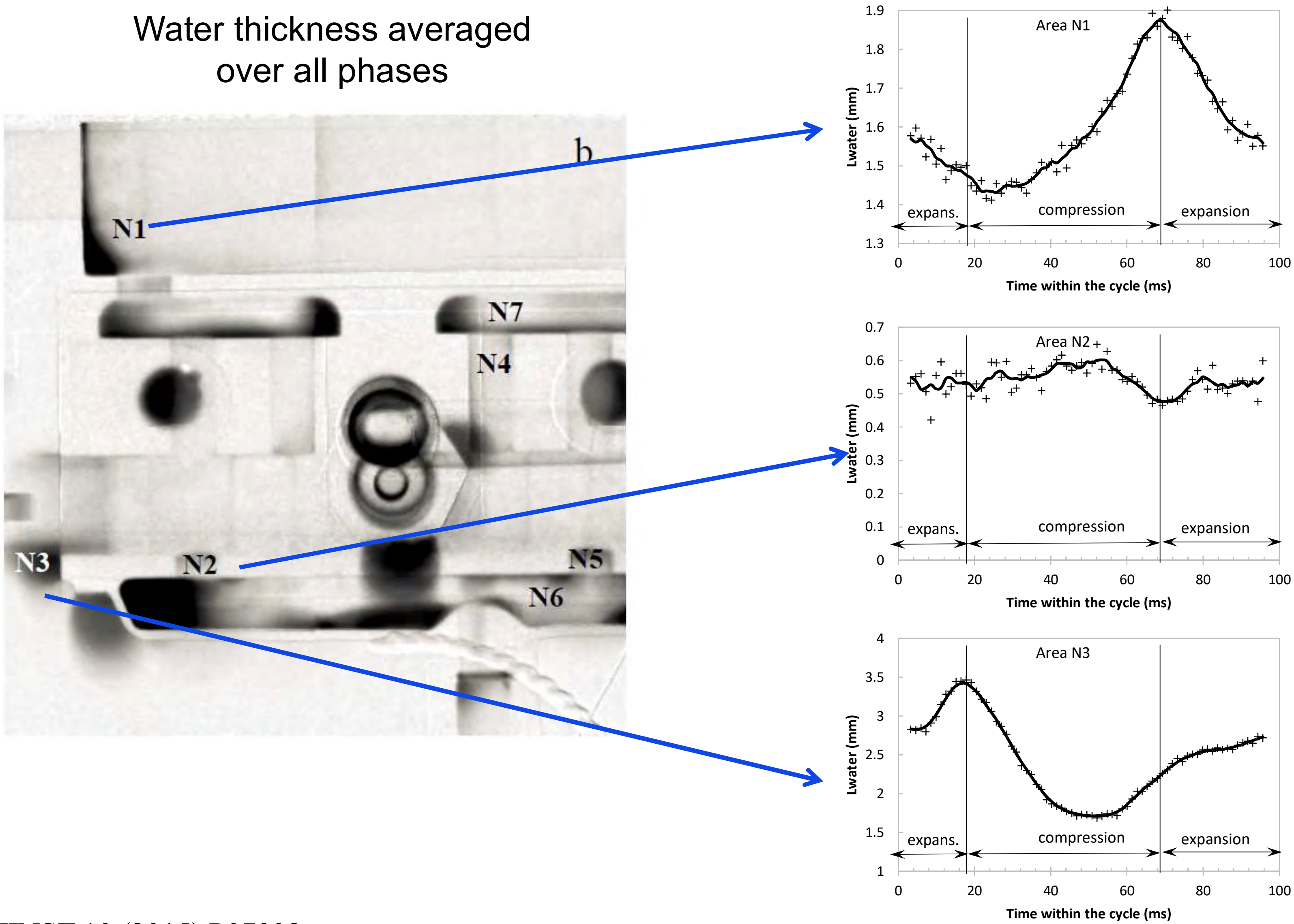

JINST 10 (2015) P07008

Dynamic imaging of magnetic fields and domain walls

All phases are measured simultaneously (unlike in stroboscopic imaging)

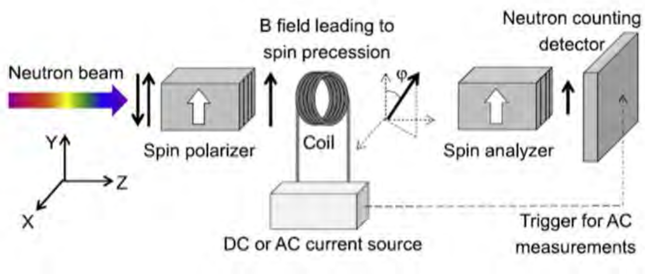

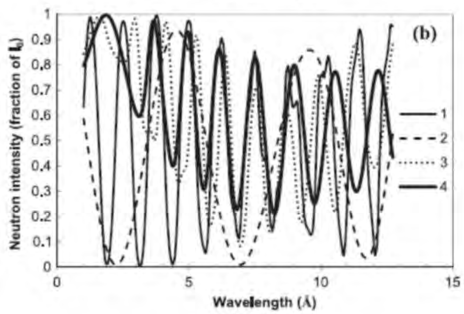

2 phase flow

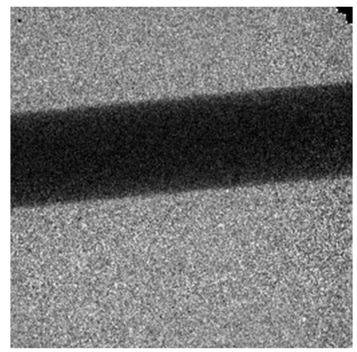

A. S. Tremsin, et al., IEEE Trans. Nucl. Sci 57 (2010) 2955

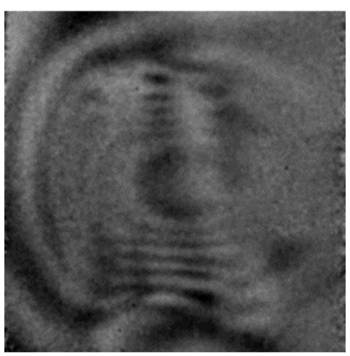

3 kHz field measured with 10 μs frames

A.S. Tremsin, et al., New Journal of Phys. **17** (2015) 043047

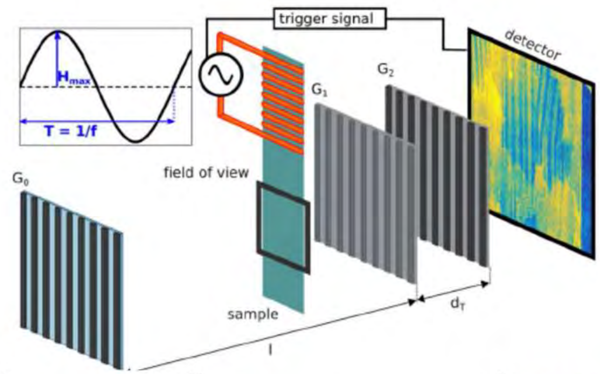

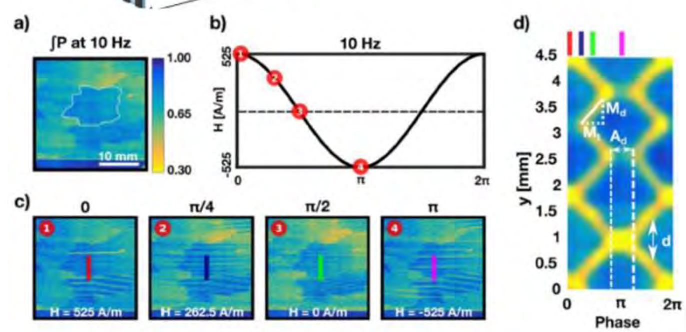

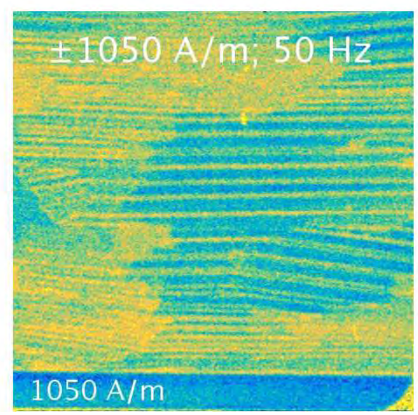

R.P. Harti, et al, Scientific Reports **8** (2018) 15754

High spatial resolution through event centroiding

Single neutron detection: Charge accumulated in each pixel

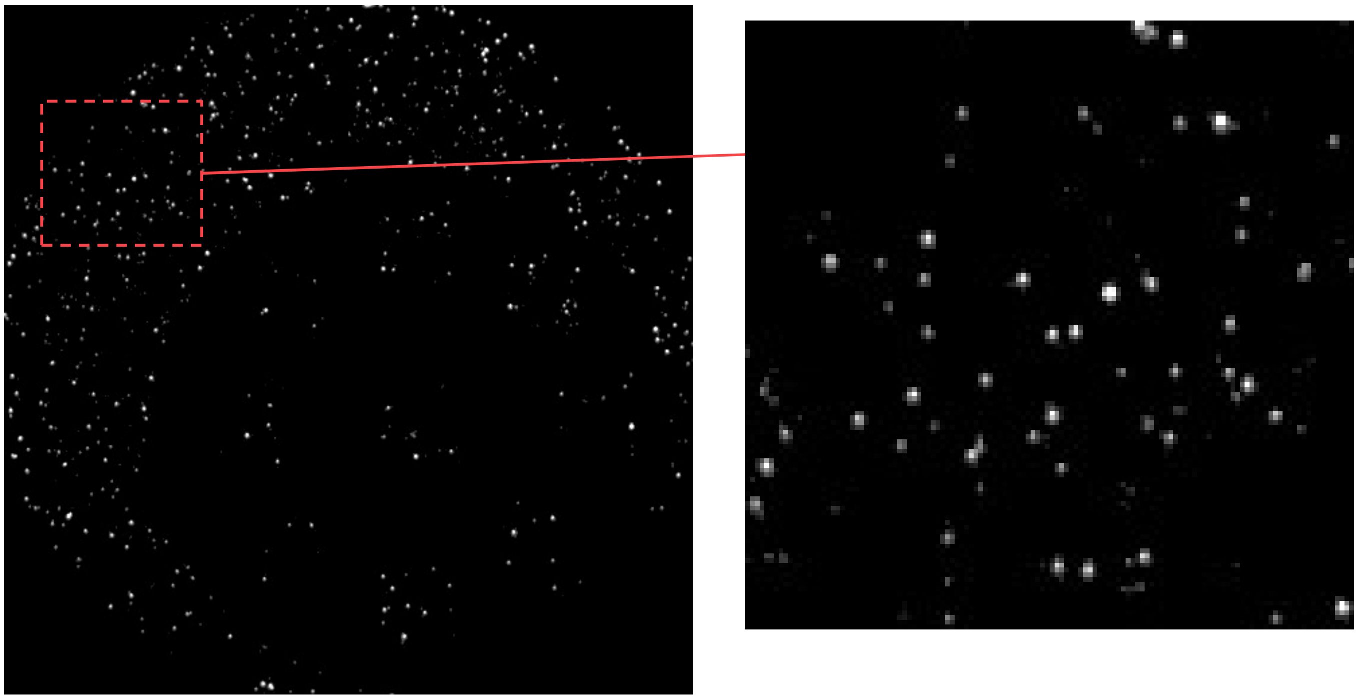

Each pixel measures charge accumulated in a frame (Time Over Threshold method)

Only one event per pixel is allowed in a frame

Single frames: event centroiding

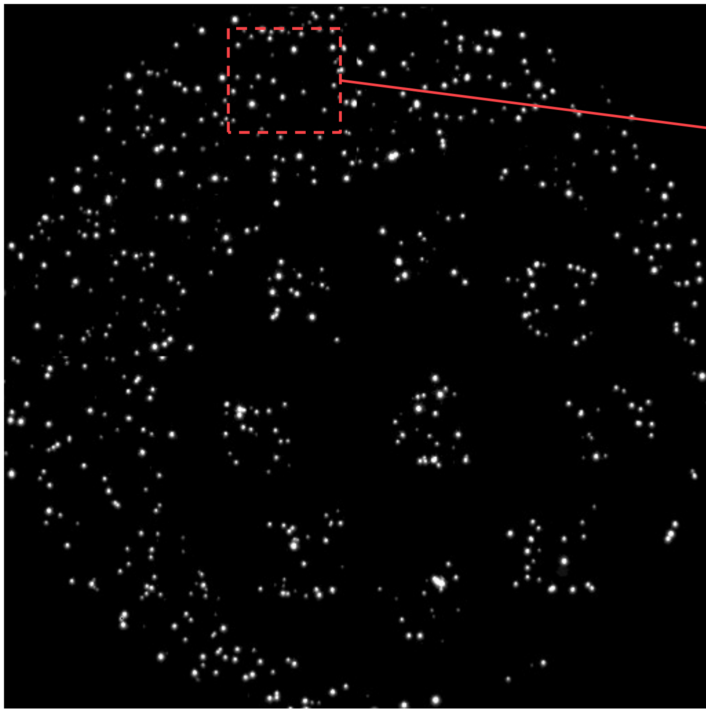

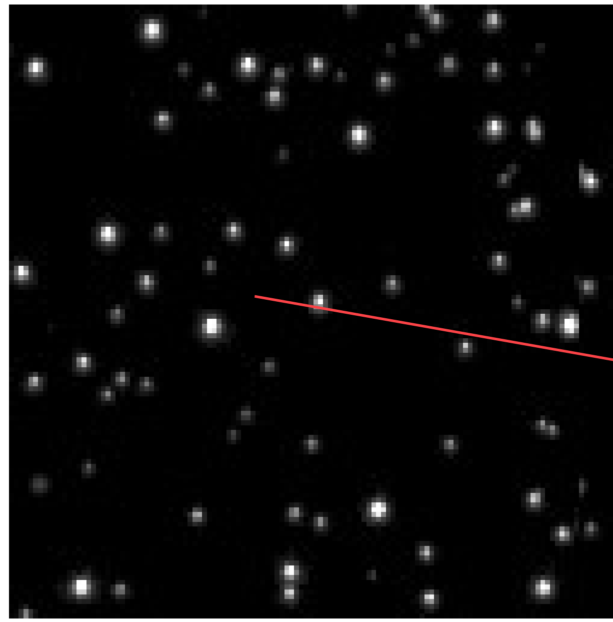

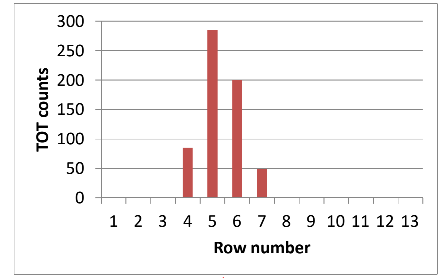

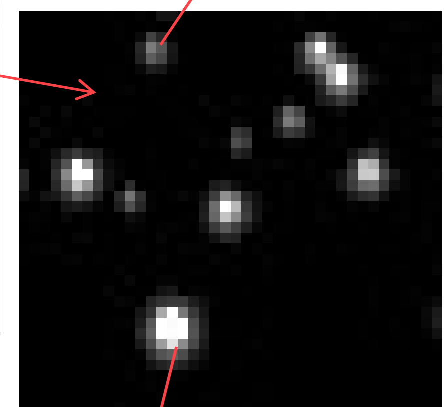

Each pixel measures charge accumulated in a frame
(Time Over Threshold method)

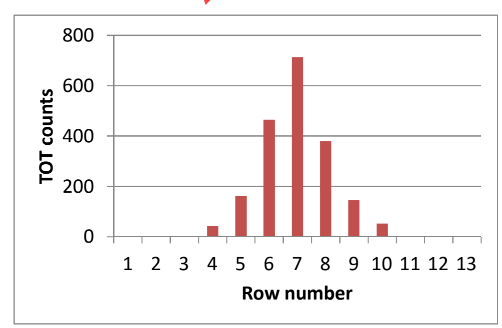

Only one event per pixel is allowed in a frame

Event centroiding for photons

High resolution imaging with up to MCP pore size is possible

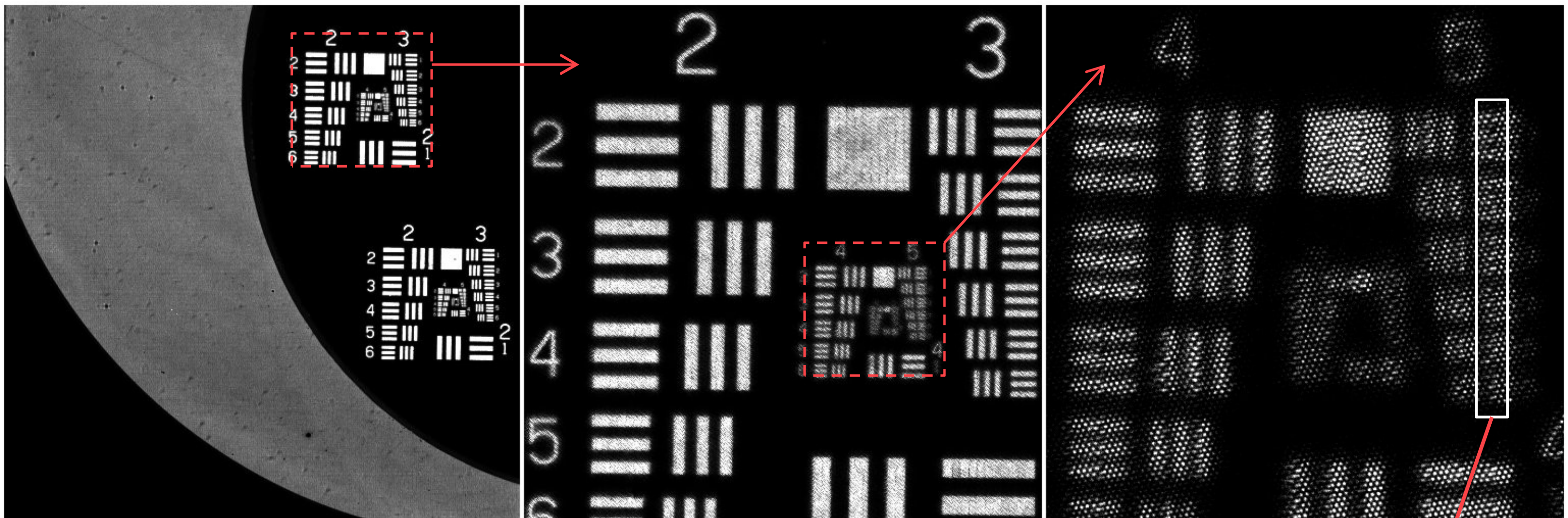

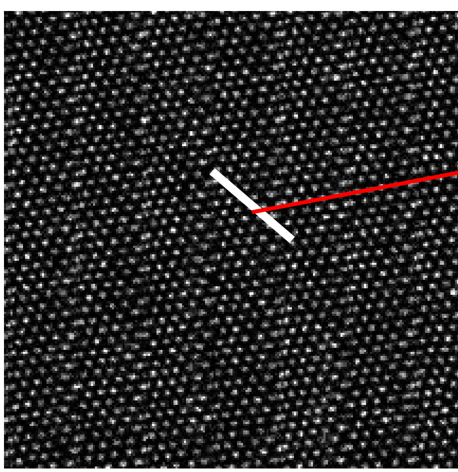

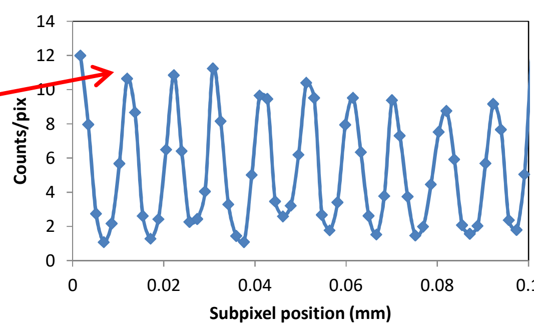

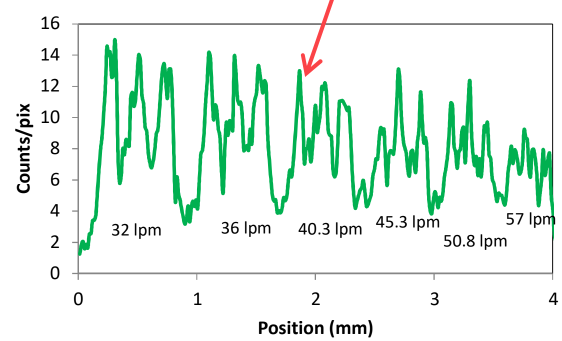

Readout resolution ~4 μm FWHM

Nucl, Instr. Meth. A 787 (2015) pp. 20-25.

High spatial resolution: event centroiding

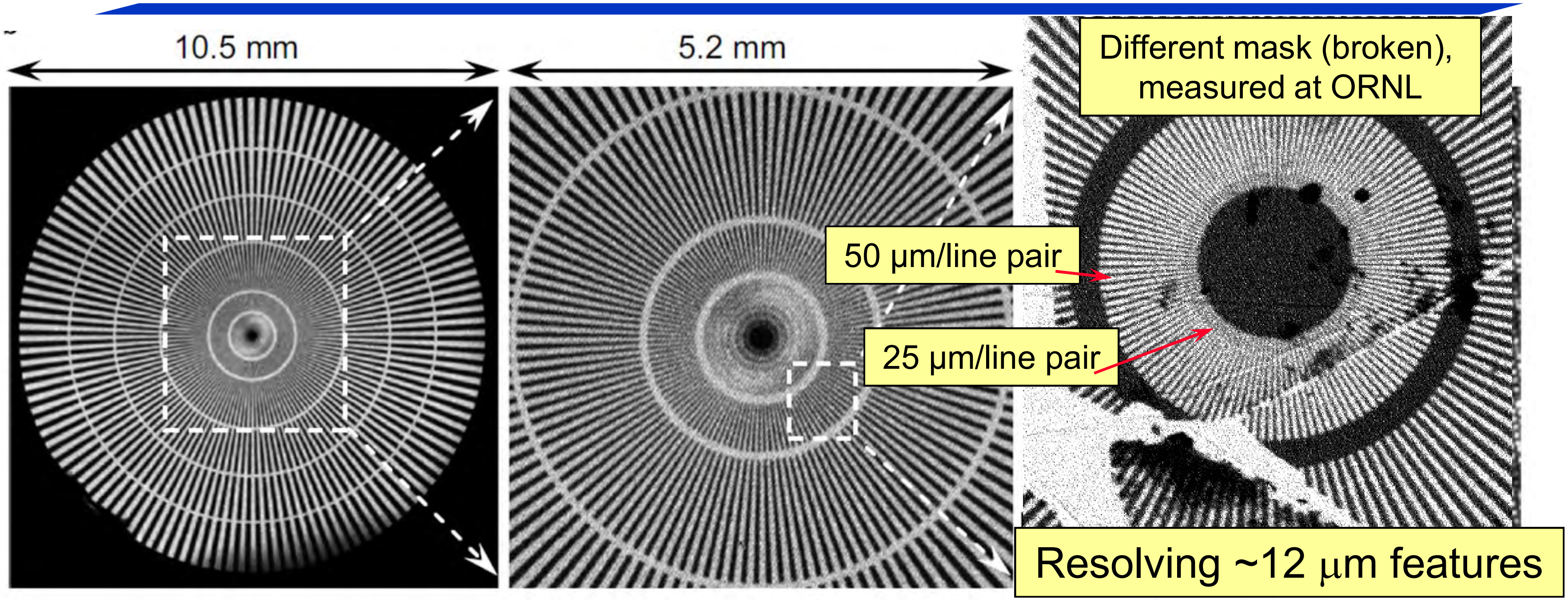

Nucl. Instr. Meth. A 784, pp. 486-493 (2015).

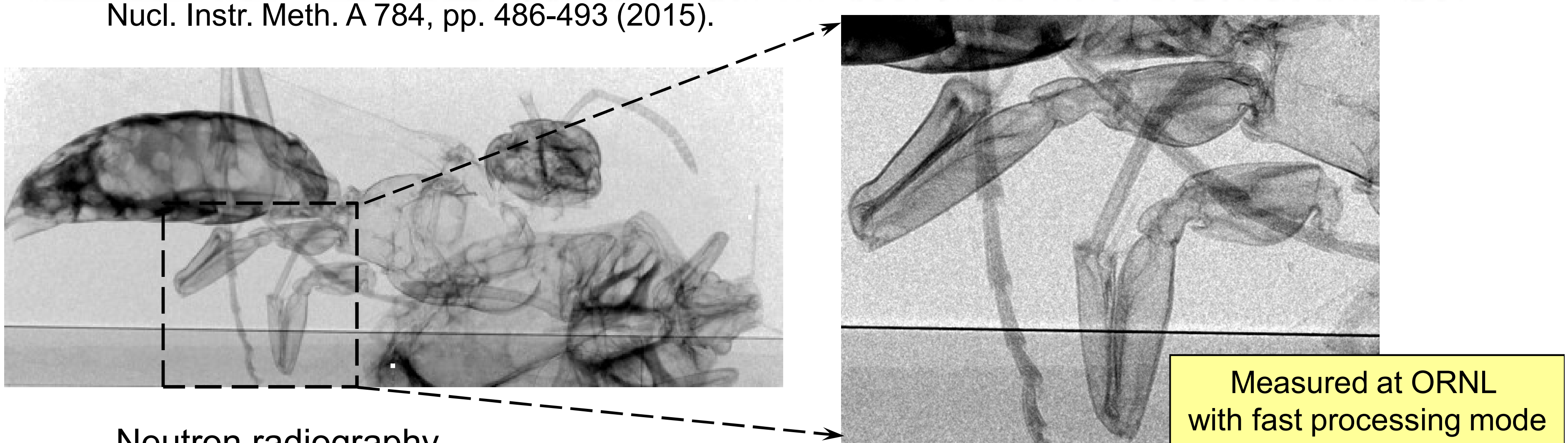

Neutron radiography.
Centroiding mode.

Energy-resolved neutron imaging: time of flight

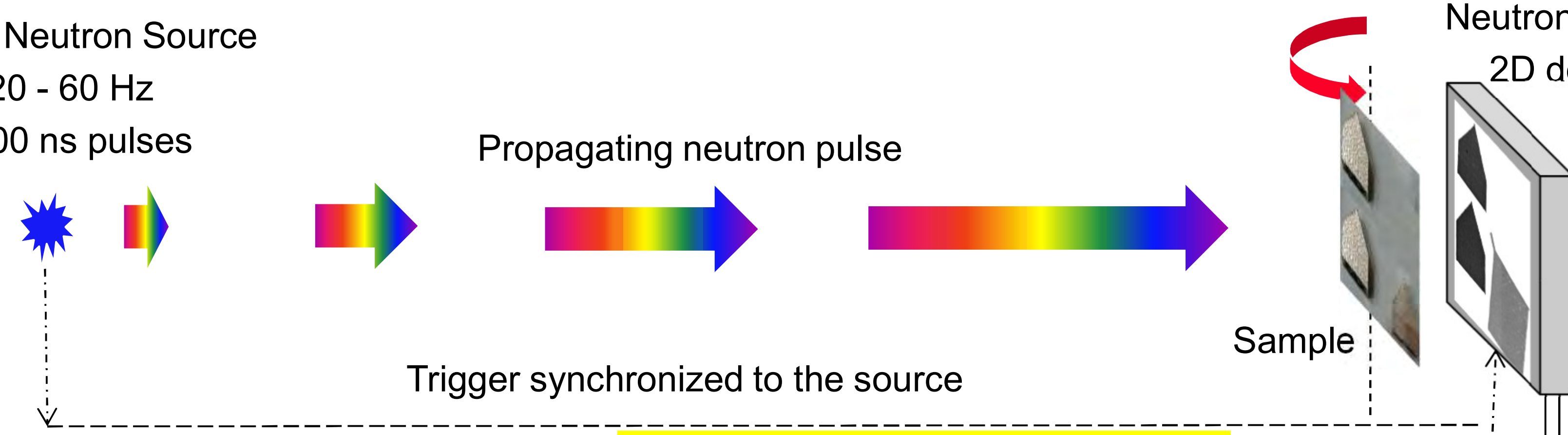

All energies are imaged at the same time!

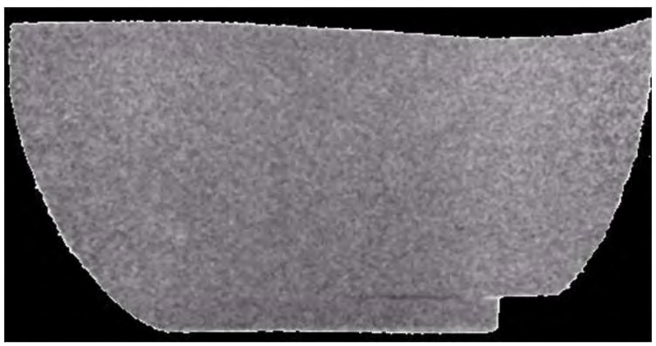

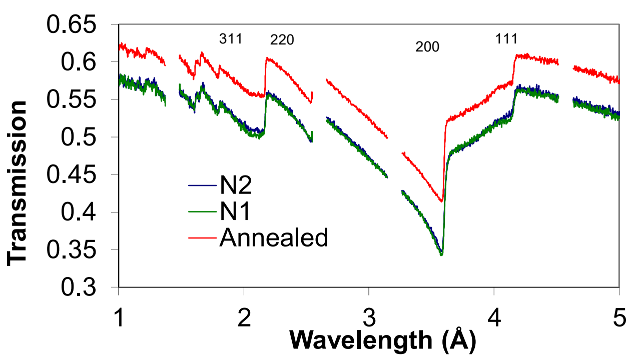

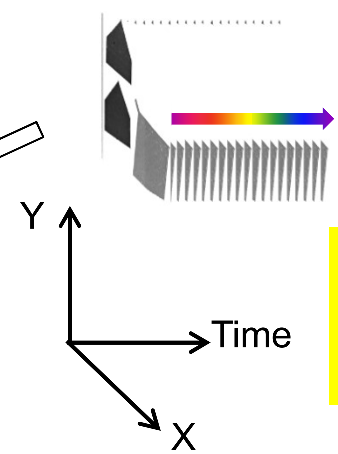

~250,000 spectra is measured simultaneously!

Plastic MCPs for fast neutron detectoin

Plastic microchannel plates for fast neutron detection

- Hydrogen-rich PMMA microchannel structure
- Graded Temperature ALD deposition
  - *Active films deposition at 140C*
- Neutron-proton recoil reaction within plastic at better than 1% efficiency
- Proton initiated secondary electron cascade
- Output pulse $10^3 – 10^6$ electrons
- Standard readout electronics
- Technology is scalable to large format

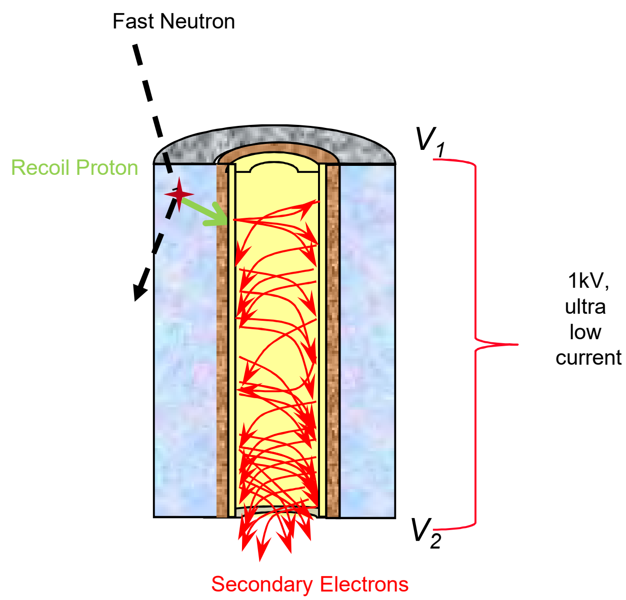

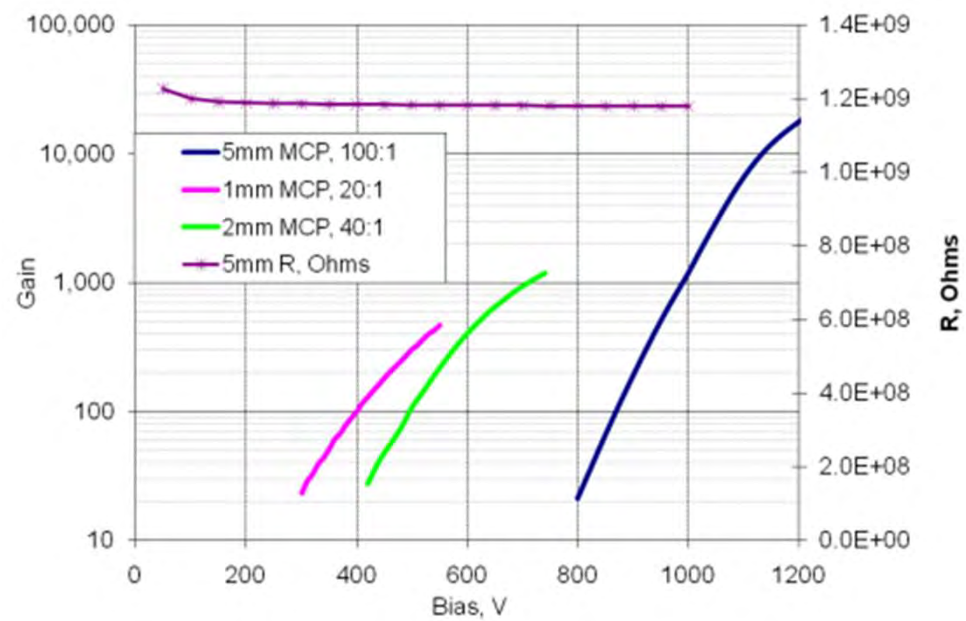

MCP manufacturing process

Current MCP Fabrication Process

Substrate Fabrication

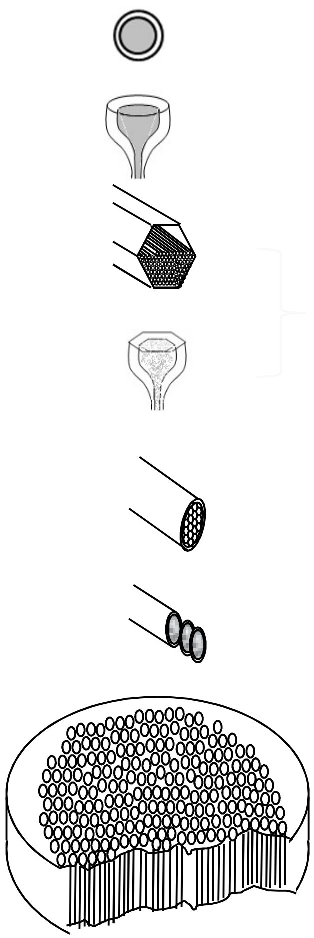

1" Etch-able Core
Lead Glass Rod

Draw Tower

Stacked
Draw Tower
Repeated

Boule
5-100mm Dia

Diced
0.2-0.3 mm thick

Etched
Producing >5M
0.002 mm pores

Substrate Functionalize

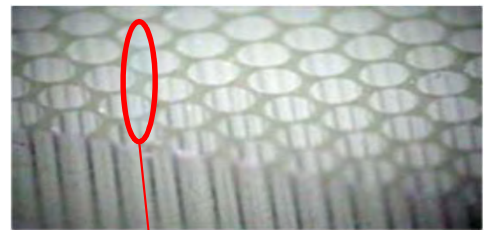

Furnace H_2 Firing
Pulls lead glass impurities to surface creating slightly conducting high SE yield surface layer

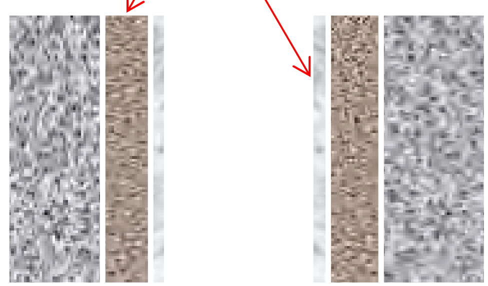

Mature (1960s) Process

- Low yield - expensive
- Bulk materials determine performance
- limited size (<10cm)

The **ALD** process replaces the **Furnace H2 Firing process**, separating the bulk substrate material from device performance

ALD Cycle for Al_2O_3

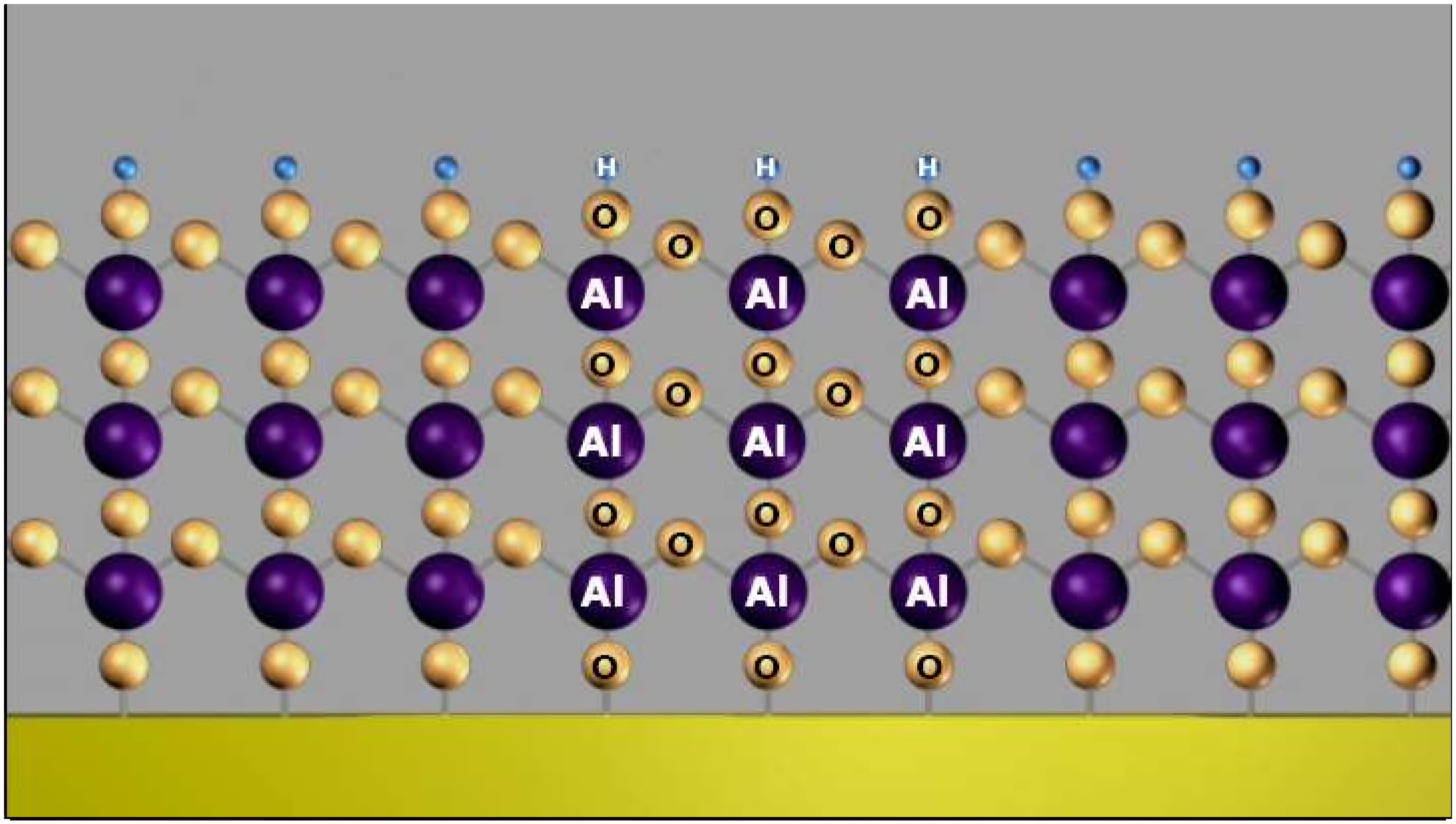

ALD Thin Film Materials

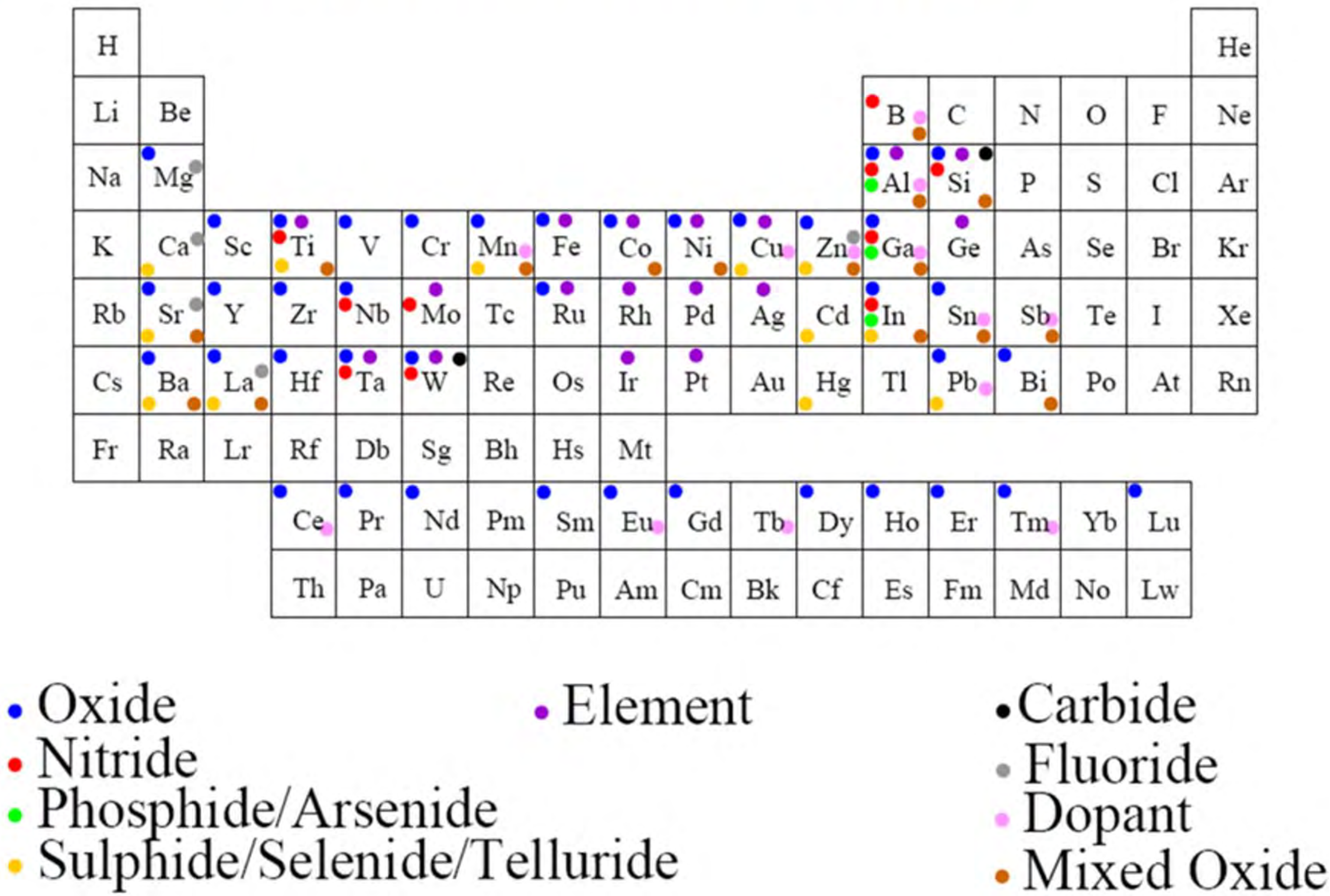

Graphic Courtesy J. Elam Argonne National Labs

ALD MCP Technology

- MCP performance tied to glass composition

ALD:

- Device optimization is de-coupled from substrate.
- Semiconductor processes & process control.
- Materials engineering at the nanoscale
- Functional films composed of abundant,non-toxic materials.
- Advantages:
  - ***<u>High conformality (>500:1)</u>***
  - *Scalable to large areas*
  - *Digital thickness control*
  - *Pure films*
  - *Control over film composition*
  - *Low deposition temperatures (50-300°C)*

- Thin film growth that relies on self-limiting surface reactions
- Gas A reacts with a surface
  - *excess precursor & reaction by-product removed.*
- Gas B is introduced to the evacuated chamber – reacts with surface bound A
  - *excess precursor & reaction by-product removed.*
- Repetition of A – B pulse sequence to build film layer-by-layer

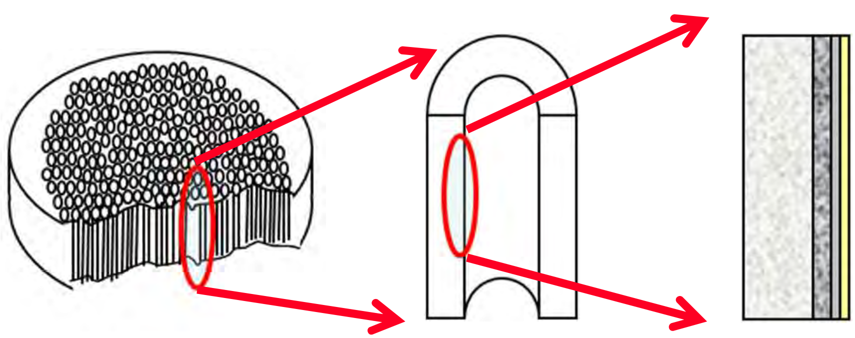

Plastic MCP: ALD resistive and conductive films

Pores ~50 µm, center to center spacing ~70 µm, L/D ratio ~20:1 and ~27:1

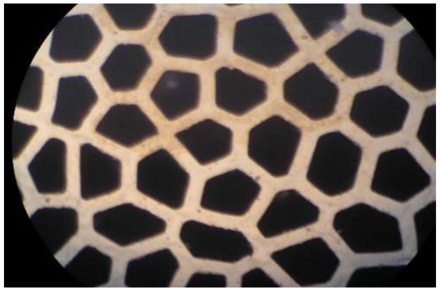

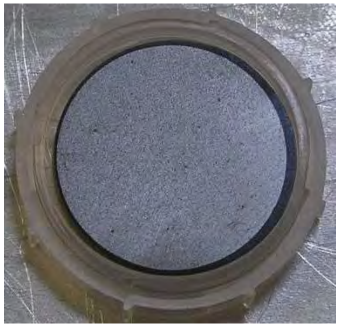
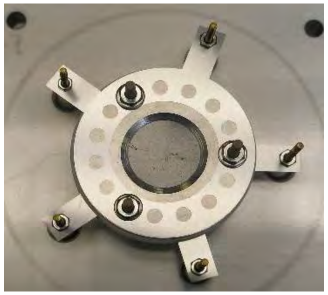

Resistive and conductive films were developed for compatibility with low temperature ALD deposition process.

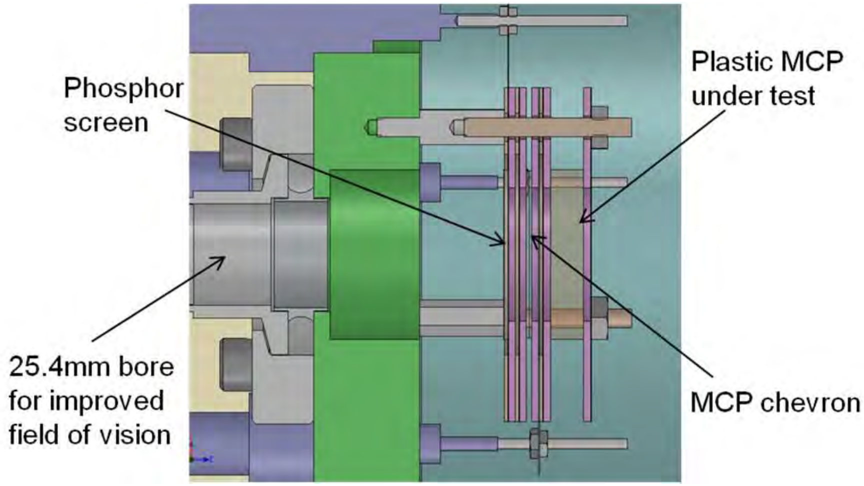

Neutron detection efficiency

$$P_{detection} = P_1 * P_2 * P_3$$

P_1 – interaction of neutron within the MCP glass

P_2 – reaction product(s) escape into MCP pore

P_3 – electron avalanche is formed (MCP ~1)

A. S. Tremsin, et al., IEEE Trans. Nucl. Sci. 52 pp.1739-1744 (2005).
A.S. Tremsin, et al., Nucl. Instrum. Meth. A 539, pp. 278-311 (2005).

Plastic MCP: probability of proton recoil P1

PMMA $(C_5\text{-}O_2\text{-}H_8)_n$

N of monomers per cm^3
7.16+21
N of H atoms per cm^3
5.73E+22
N of C atoms per cm^3
3.58E+22
N of O atoms per cm^3
1.43E+22

$$P = [1 - \exp(-N_i\, \sigma_i\, L)](1-A)$$

Cross section of neutron interaction

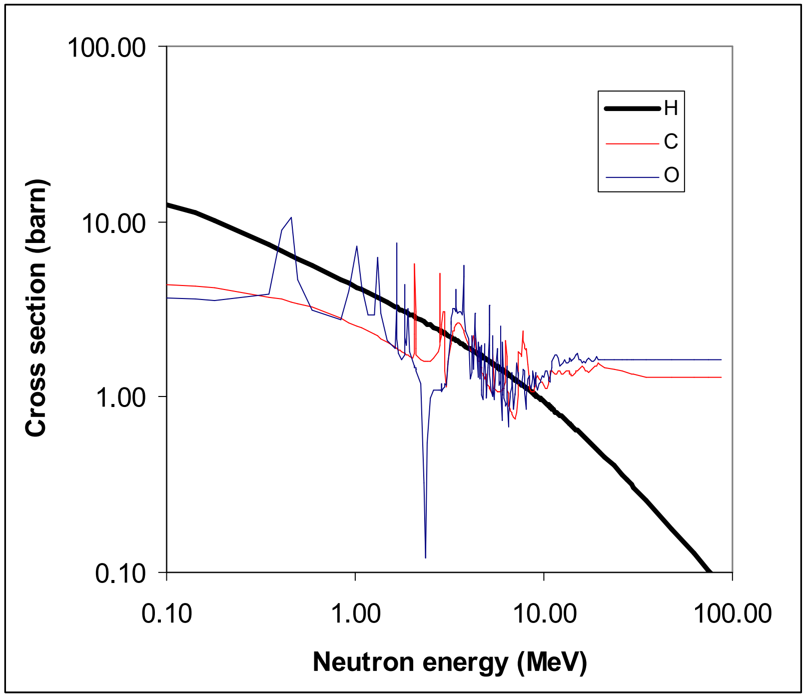

Plastic MCP: probability of proton recoil P1

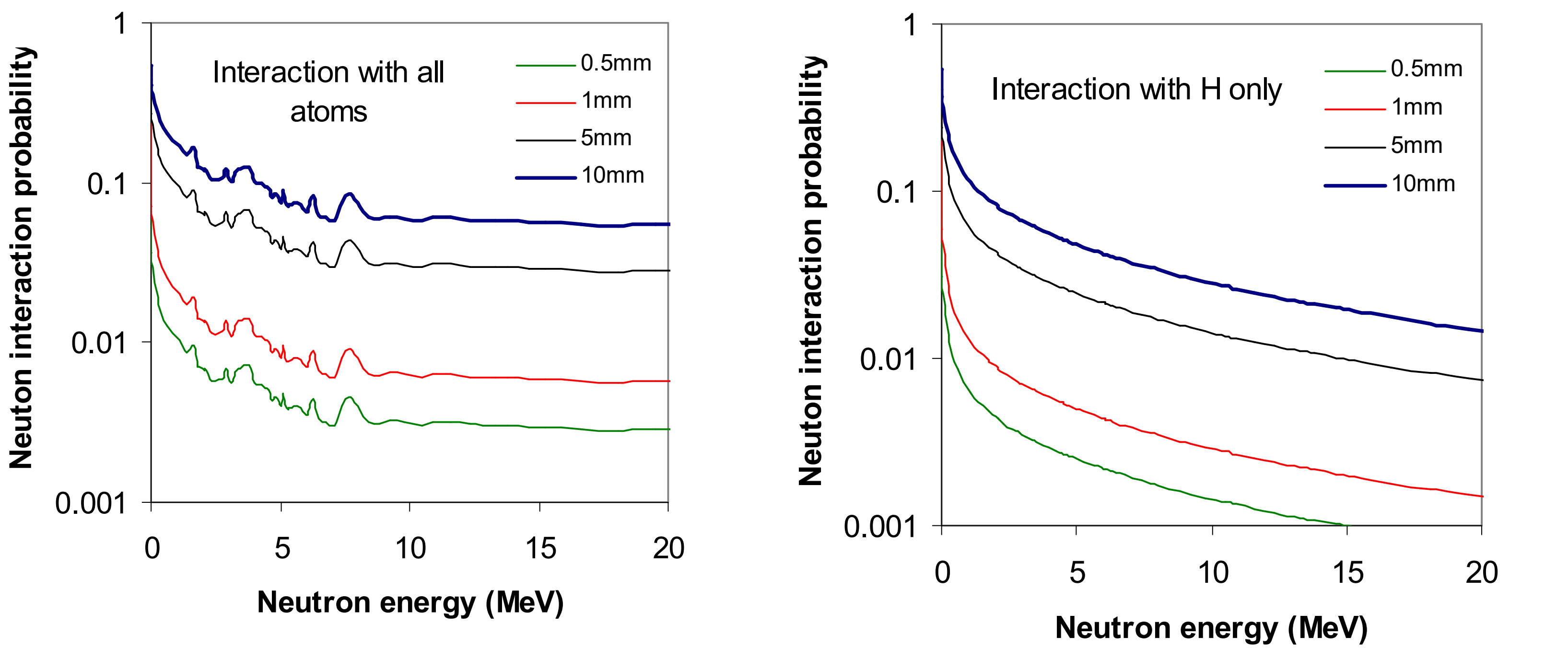

PMMA $(C_5\text{-}O_2\text{-}H_8)_n$

50 µm circular pores, 20 µm walls, 1.19 g/cm^3

Recoil proton escape probability P_2

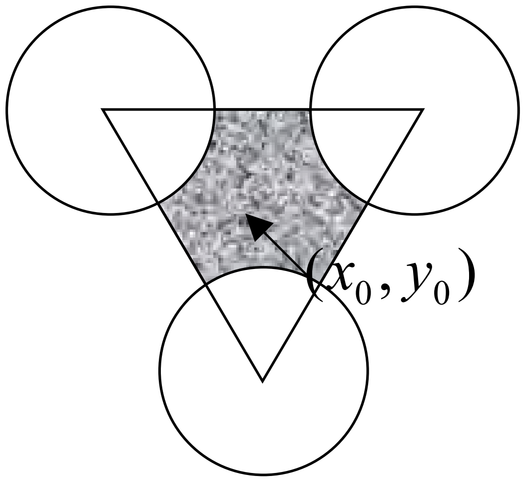

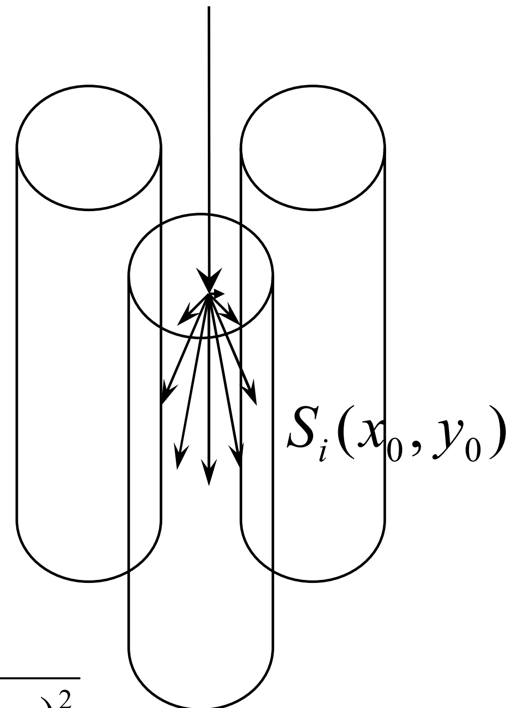

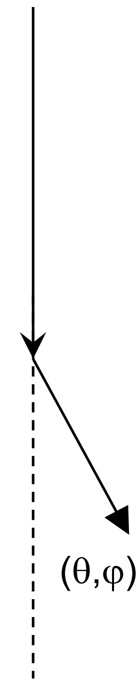

$$\cos(\theta) = \sqrt{\frac{E_p}{E_n}}$$

$E_p \in [0, E_n]$

$$S_i(x_0, y_0) < R(E_p(\theta))$$

$$S_i(x_0, y_0) = \frac{\sqrt{(x_1 - x_0)^2 + (y_1 - y_0)^2}}{\sin(\theta)}; \theta \neq 0, \pi$$

$$\xi = y_0 - tg(\varphi)x_0 - O_{i,y}$$

$$(x_1 - x_0)^2 = \left[\min\left|\left\{-\left(tg(\varphi)\cdot\xi - 0_{i,x}\right) \pm \sqrt{D}\right\}\cos^2(\varphi) - x_0\right|\right]^2$$

$$y_1 = tg(\varphi)\cdot x_1 + \left(y_0 - tg(\varphi)x_0\right)$$

$$D = \left(tg(\varphi)\cdot\xi - O_{i,x}\right)^2 - \left(O_{i,x} + \xi^2 - \frac{d^2}{4}\right)^2 \frac{1}{\cos^2(\varphi)}$$

Recoil proton escape probability P_2

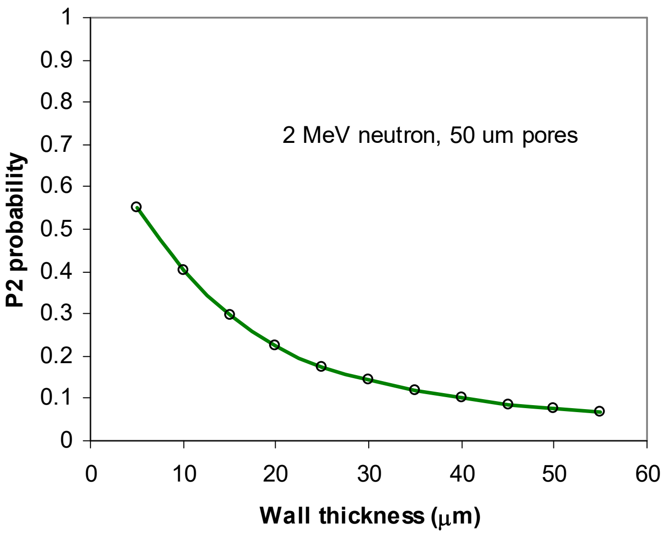

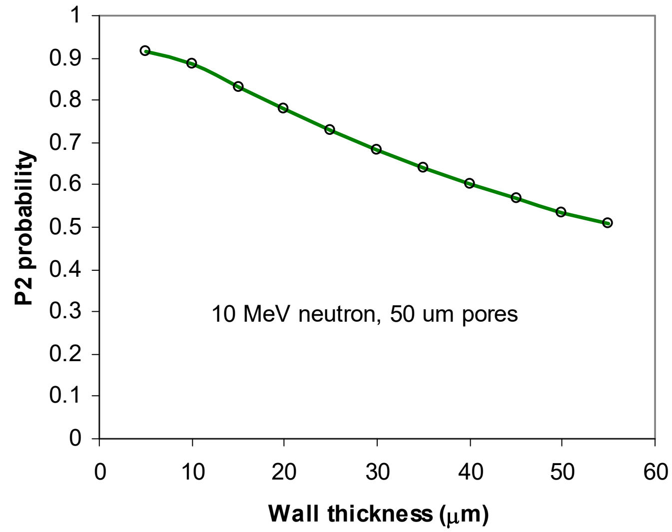

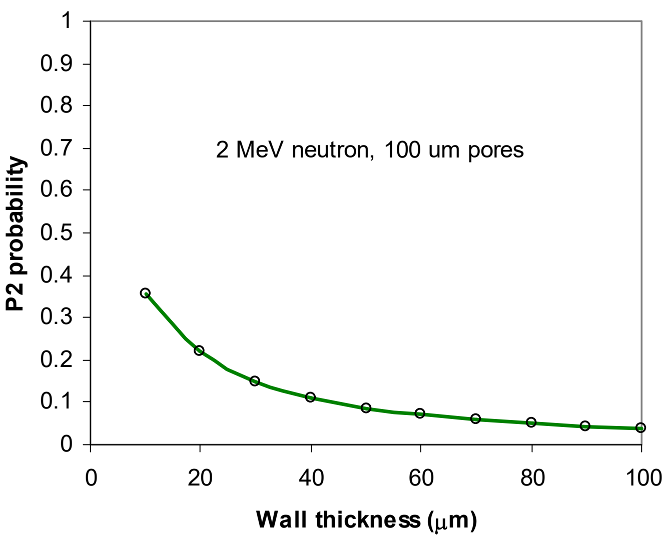

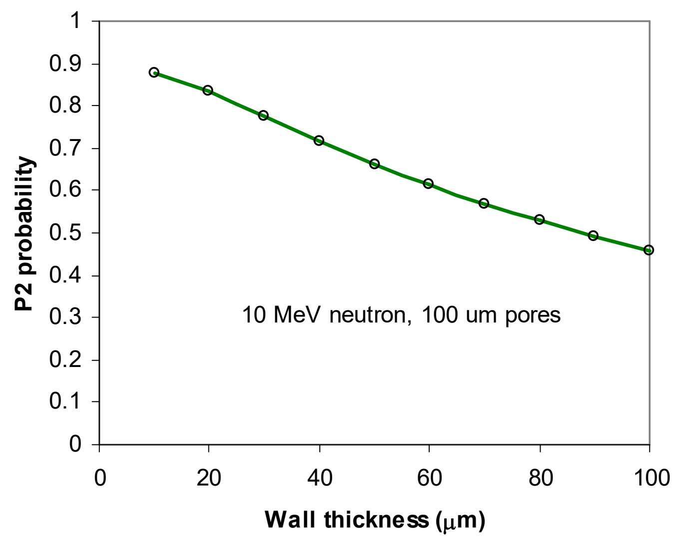

$P_1 \times P_2$

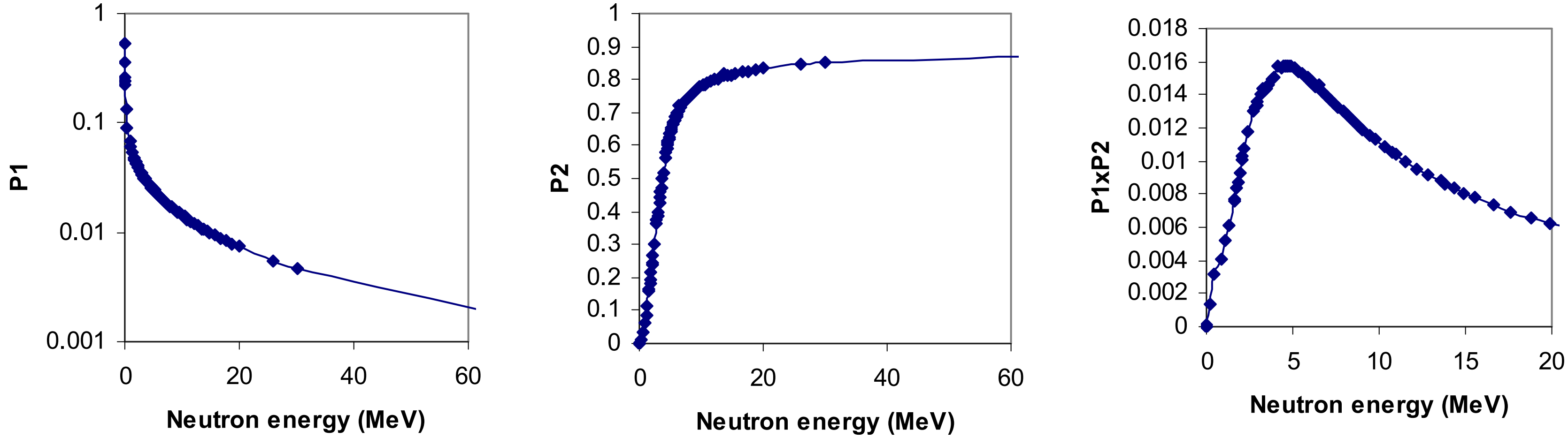

50 um pores and 20 um walls, 5 mm thick

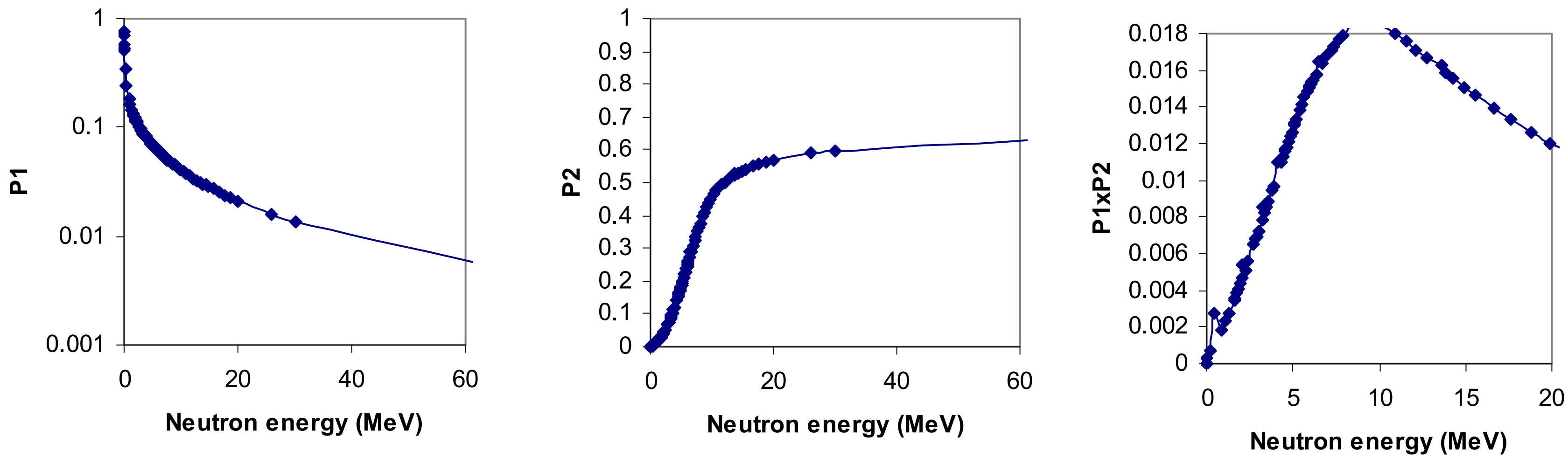

100 um pores and 100 um walls, 10 mm thick

Detector Hardware Experimental Setup

- 2 & 5 mm PMMA MCP, ~50 µm pores, 20 µm walls, 5^o bias angle
- installed above a chevron stack of 50:1 L/D MCPs
- Phosphor screen readout
- Canberra preamp and post amplifier

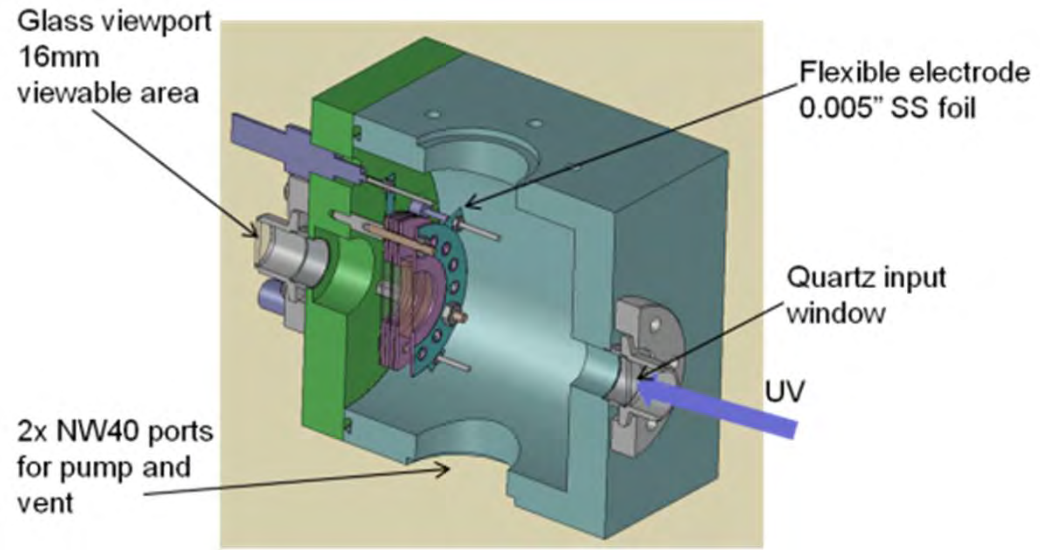

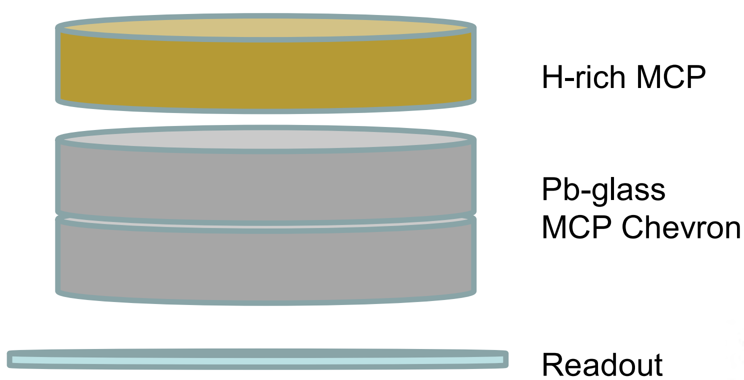

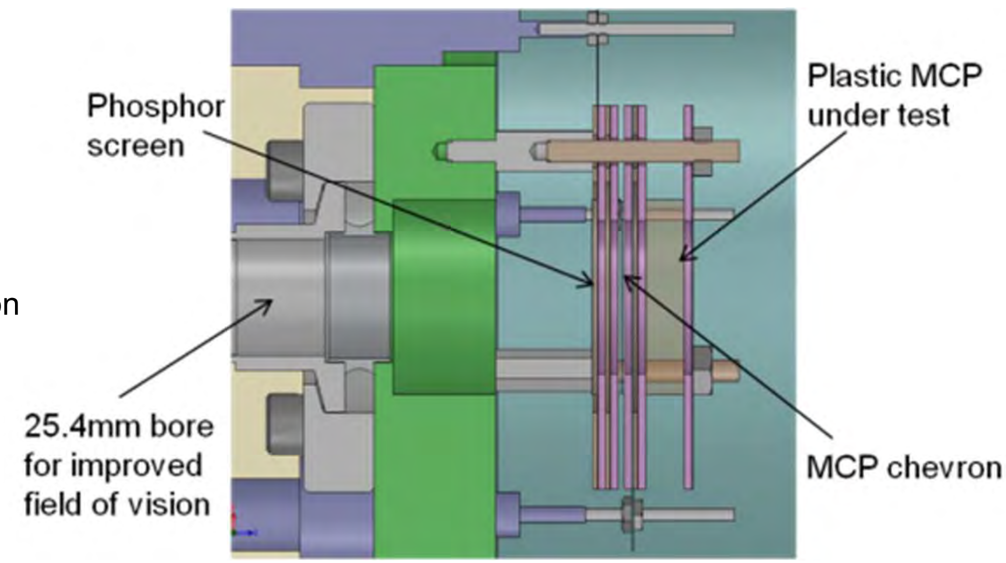

D-T Source (Thermo 320) Experimental Setup

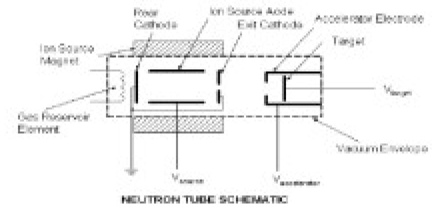

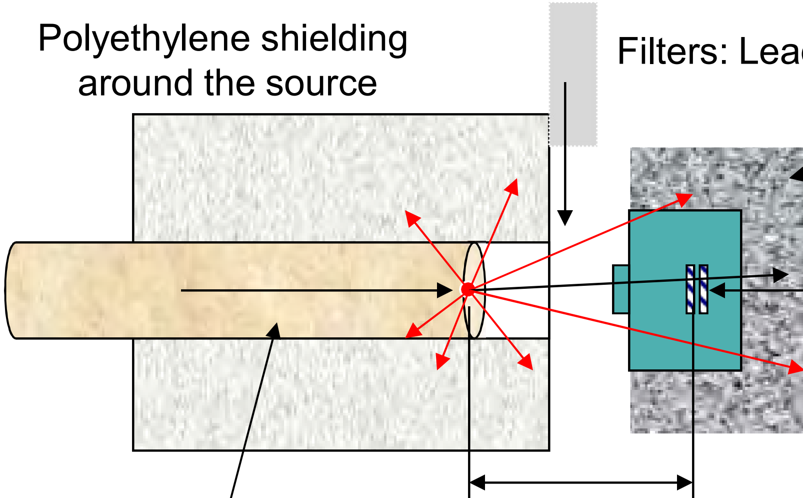

5 mm PMMA MCP,
~50 µm pores, 20 µm walls, 5º bias angle
installed above a chevron stack
of 50:1 L/D MCPs

Technical Specifications	
Neutron Yield	1.0E+08 n/s
Neutron Energy	14 MeV
Typical Lifetime	1,200 hours @ 1x10^8 n/s
Pulse Rate	250 Hz to 20 kHz, continuous
Duty Factor	5% to 100%
Minimum Pulse Width	5 µsec
Pulse Rise Time	Less than 1.5 µsec
Pulse Fall Time	Less than 1.5 µsec
Maximum Accelerator Voltage	95 kV
Beam Current	60 µamps

Coincidence gamma rejection through TOF

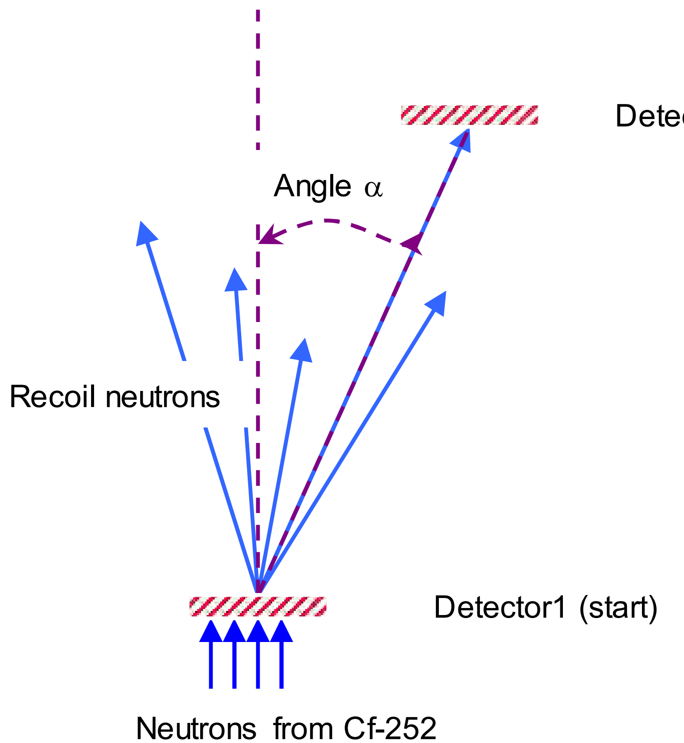

Gamma photons travel with the speed of light – detection in two detectors happens within ~1 ns

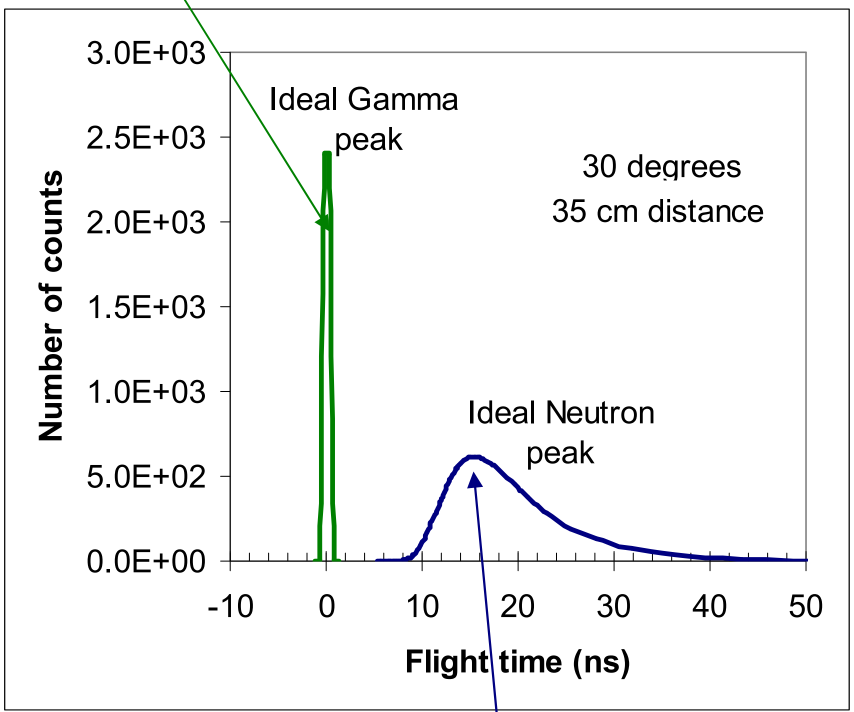

Recoil neutrons (colder than original Cf-252 spectrum) arrive with a delay dT to detector2

Coincidence measurements with Cf-252

Coincidence measurements for time of neutron flight

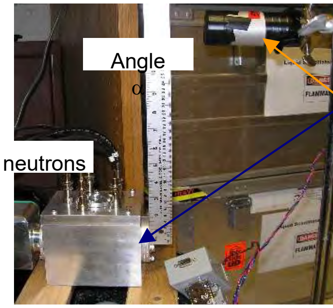

Plastic MCP detector
(start signal at TAC)

Liquid scintillator detector (BC519)
(stop signal at TAC)

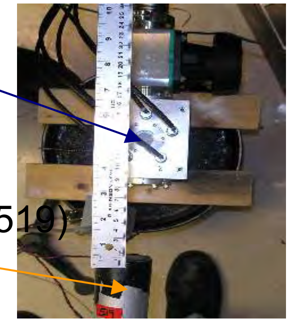

Neutrons from Cf-252

20 cm separation

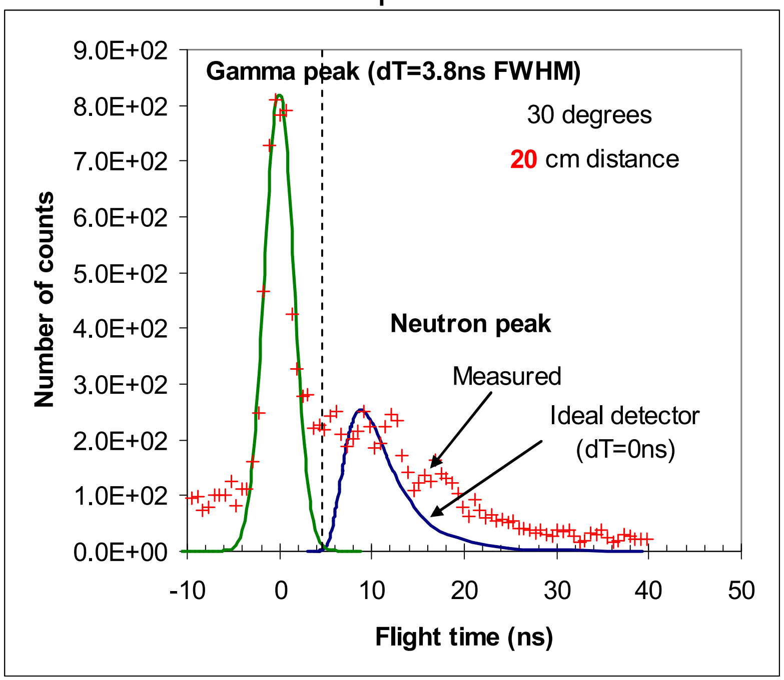

35 cm separation

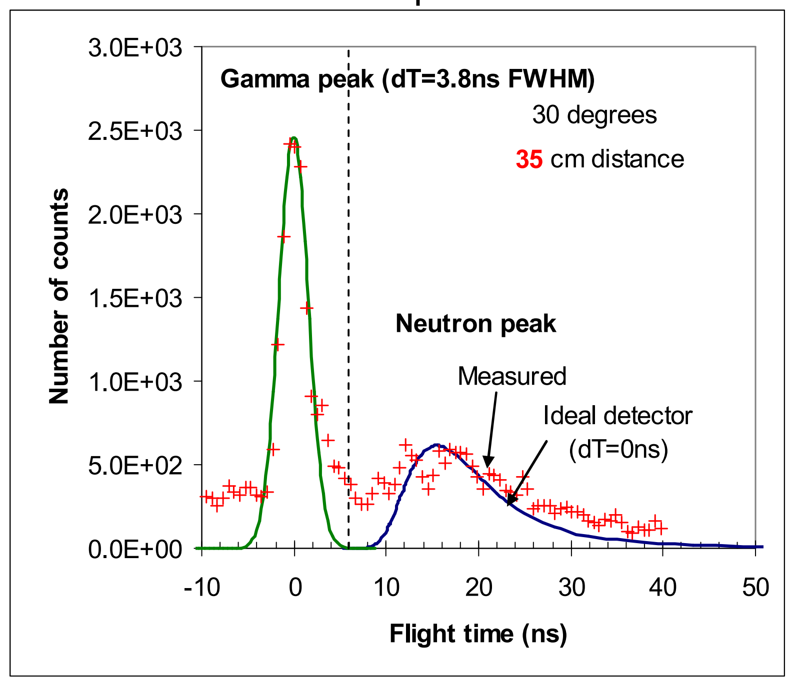

Some results on plastic MCP have been published

Contents lists available at SciVerse ScienceDirect

Nuclear Instruments and Methods in Physics Research A

journal homepage: www.elsevier.com/locate/nima

Timing resolution of fast neutron and gamma counting with plastic microchannel plates

D.R. Beaulieu[a], D. Gorelikov[a], H. Klotzsch[a], J. Legere[b], J. Ryan[b], P. de Rouffignac[a], K. Saadatmand[a], K. Stenton[a], N. Sullivan[a], A.S. Tremsin[a,*]

[a] Arradiance, Inc., 142 North Road, Sudbury, MA 01776, USA
[b] Space Science Center, 330 Morse Hall, 8 College Road, University of New Hampshire, Durham, NH 03824, USA

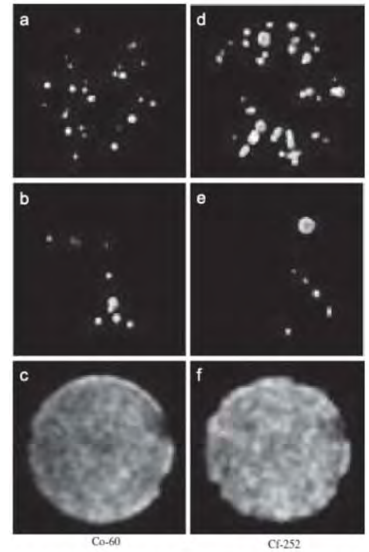

Fig. 4. Phosphor screen images of events detected with Co-60 gamma source (a)–(c) and Cf-252 gamma and neutron source (d)–(f). The individual events are seen in images (a),(d) ~99 ms integration time and (b),(e) ~33 ms integration time. The large distance between the phosphor screen and MCP led to substantial charge spread, which can be used for event centroiding. High spatial resolution in "image intensifier" mode will require short distance between the phosphor and MCPs. The image (c) was accumulated over 62 s and has ~11300 detected gamma photons from Co-60 source, while image (f) was integrated over 22.8 s and contains ~5000 events (produced by both gamma and fast neutrons).

Contents lists available at ScienceDirect

Nuclear Instruments and Methods in Physics Research A

journal homepage: www.elsevier.com/locate/nima

Plastic microchannel plates with nano-engineered films

D.R. Beaulieu, D. Gorelikov, H. Klotzsch, P. de Rouffignac, K. Saadatmand, K. Stenton, N. Sullivan, A.S. Tremsin*

Arradiance, Inc., 142 North Road, Sudbury, MA 01776, USA

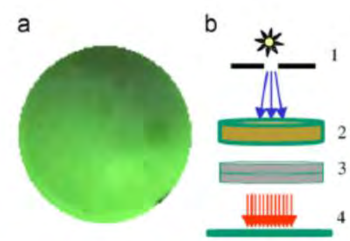

Fig. 4. (a) Photograph of the phosphor screen with detector under UV illumination. No noise spots or artifacts from PMMA MCP are observed. The defects on the image are due to the phosphor internal features. (b) Schematic diagram of the pulse counting detector configuration (not to scale). 1—UV light source with an aperture, 2—PMMA MCP, 3—standard lead glass MCP (or a chevron stack) used for post-amplification of electron signal produced by the PMMA MCP and 4—phosphor screen/charge collecting anode.

Thank you for your attention!

This work was done within the Medipix collaboration.

We would like to thank Medipix collaboration for the readout electronics and data acquisition software (Advacam, Prague and Espoo, NIKHEF, Amsterdam and IEAP, Prague).

This work was supported in part by U.S. agencies: NASA, DOE, NSF, NIH and NNSA.